JOTCS A
Journal of the Turkish Chemical Society
Section: A
Chemistry
TURKISH CHEMICAL SOCIETY

Preparation of PLGA-PEG/Hydroxyapatite Composites via Simple Methodology of Film Formation and Assessment of Their Structural, Thermal, and Biological Features

Fatih Ciftci[1*], Ali Can Özarslan[2]

[1]Department of Biomedical Engineering, Fatih Sultan Mehmet Vakif University, Istanbul, 34445, Turkey.
[2]Faculty of Chemistry Metallurgy, Department of Bioengineering, Yildiz Technical University, Istanbul, 34220, Turkey.

Abstract: This study aimed to develop polymeric composite films suitable for applications in the field of bone tissue engineering. The preparation of PLGA-PEG/HAP composite films was achieved using a simple methodology, including mixing, sonication, and casting-drying stages. Characterization analyses, including FTIR, SEM, TGA-DSC, and XRD, were conducted to assess the properties of the composite films. The results showed that the PEG polymer decreased the glass transition temperature of the composite, while the HAP did not change. Further, weight remaining (%) values of HAP, PLGA-PEG, and PLGA-PEG/HAP were found as 94.04, 88.28, and 90.57, respectively. Thus, it can be concluded that HAP improves the thermal stability of PLGA-PEG. The outcomes of the analysis, encompassing the evaluation of physical, morphological, and thermal properties, demonstrate that the composite structure comprising PLGA and PEG polymers along with HAP ceramic material may attain the intended quality. Moreover, fluorescence microscopy was employed to visualize the interaction between cells and the composite films following DAPI staining to evaluate cell adhesion and proliferation on the PLGA-PEG/HAP composite films. PLGA-PEG/HAP composite films have no adverse effects on cells, such as toxicity, and they have also exhibited a favorable influence on cell proliferation, supporting an augmentation in cellular growth and adhesion. Overall, the results indicate that the synthesized PLGA-PEG/HAP composite films may hold the potential to serve as a promising candidate for applications in the field of bone tissue engineering.

Keywords: Bone tissue engineering, PLGA, PEG, Hydroxyapatite, Composite, Film.

Submitted: June 12, 2023. **Accepted:** September 30, 2023.

Cite this: Ciftci F, Özarslan AC. Preparation of PLGA-PEG/Hydroxyapatite Composites via Simple Methodology of Film Formation and Assessment of Their Structural, Thermal, and Biological Features. JOTCSA. 2023;10(4):1123-32.

DOI: https://doi.org/10.18596/jotcsa.1313562

***Corresponding author's E-mail:** faciftcii@gmail.com

1. INTRODUCTION

Tissue engineering is an emerging field in biomaterial research with great therapeutic potential (1). Recent studies in the treatment of spinal cord injury have utilized tissue engineering technology, particularly for the design of a biological scaffold containing polymers, support cells and growth factors (2). We have investigated a three-dimensional tissue scaffold that can mimic the properties of the spinal cord to enable axonal regeneration in spinal cord injury (3). When placed in the damaged area, this scaffold needs to be orientated along the injured area to regenerate neuronal tissue and provide adequate mechanical support for regenerating nerve fibers (4). An ideal neural scaffold should be biocompatible, biodegradable to avoid toxicity, permeable for nutrient and gas exchange, and have sufficient mechanical strength (5). The scaffold should gain elasticity to reduce stress at the injured point. The balance between the flexibility and rigidity of the scaffold should also be well balanced. Excessively hard scaffolds may dislodge easily, while overly soft ones may not support axonal regeneration (6).

The use of synthetic polymers instead of natural polymers in scaffolding offers a wider scope for designing and controlling the properties of the material. The most commonly used synthetic polymers in the spinal cord are either polyester-

based biodegradable materials such as PLA and PGA, or biodegradable hydrogels based on PEG. PLGA, a copolymer of PLA and PGA, was preferred as a synthetic polymer (5). This material is biocompatible and biodegradable. The degradation of PLGA produces glycolic and lactic acids that lower the pH and may inhibit the tissue repair process. Studies have shown that PLGA promotes axonal regeneration in nerve canals (5,7).

Poly (lactic-co-glycolic acid) (PLGA), a synthetic blend comprising polylactic acid and polyglycolic acid, is both biocompatible and biodegradable (8). Adjusting the proportion of polylactic acid to polyglycolic acid allows for control over the rate of copolymer degradation (9). PLGA-based neural conduits were inserted into fully severed rat spinal cords, resulting in observed axonal regeneration within these nerve conduits (10). However, it was noted that the degradation of PLGA produces glycolic and lactic acids, subsequently lowering the local pH and potentially hindering the tissue repair process (11).

PEG is a water-soluble compound belonging to the polyether family, known for its non-toxic nature and resistance to protein adsorption and cell adhesion (12). These characteristics make PEG a polymer that remains largely unrecognizable by the immune system upon implantation. Furthermore, PEG assists in sealing cell membranes post-injury. By manipulating the cross-links, PEG hydrogels can be tailored to degrade at various rates and employed as carriers for drug delivery (13). Additionally, they can be modified to promote improved cell adhesion (14). PEG possesses exceptional attributes for spinal cord repair, such as high hydrophilicity, biocompatibility, lack of immunogenicity, and neuroprotective qualities (15). Nevertheless, the degradation of PEG within the body hinges on the specific polyether structure. For instance, Mahoney et al. synthesized hydrolysable PEG hydrogels that were enhanced with poly (lactic acid) (PLA) and poly (glycolic acid) (PGA) (16). These PEG hydrogels exhibited remarkable resistance to protein adsorption, which can be attributed to properties like neutrality and enhanced mobility.

Hydroxyapatite (HAP) is the main inorganic component of natural bone. HAP has properties such as being biocompatible, bioactive (the ability to form direct chemical bonds with surrounding tissues), osteoconductive, non-toxic, non-inflammatory, and non-immunogenic (17). HAP is one of the ideal materials widely used in bone tissue engineering due to its biocompatibility and mechanical strength (18,19). The degradation rate of HAP implants must match the regeneration rate of native tissue and this is currently one of the biggest challenges in this field. Another purpose of using HAP is its excellent biocompatibility in soft tissue regeneration (17). Studies have shown that HAP forms a scaffold that supports the growth of fibroblasts. This in turn produces and deposits new collagen, a natural volumizing substance. Hydroxyapatite degradation is synchronized with neo-collagen deposition at the injection site, providing a lasting, natural, complete and new appearance. The use of HAP in the scaffold promotes the growth of fibroblast cells, allowing the injured area to heal and gain a new appearance (20).

Both polymers and ceramics hold individual merit as viable biomaterials, while concurrently, researchers are exploring the potential of composite materials, including polymer-polymer and polymer-ceramic blends, as promising candidates within the biomaterial domain. The composite biomaterials paradigm exhibits versatility by encompassing different production methodologies to fabricate the constituent polymers and/or ceramics. The resultant diversity in fabrication techniques may enable various forms of these materials and, moreover, can help create new materials that exhibit different properties (21). Scaffaro et al. (22) undertook the fabrication of biocomposite nanofiber scaffolds employing a combination of polycaprolactone (PCL) and graphene oxide (GO) via the electrospinning methodology. Their investigation encompassed an exhaustive evaluation, encompassing morphological and mechanical analyses, aimed at providing an in-depth understanding of the structural influence and reinforcing efficacy introduced by GO within these scaffolds. The study revealed that the diameter of PLA/GO electrospun nanofibers decreased with increased filler content, while GO-g-PEG increased the diameter. Both nanofillers enhanced PCL hydrophilicity, with PCL/GO-g-PEG showing better wettability. The addition of GO improved Young's modulus, especially when GO was surface grafted with PEG at lower concentrations. This indicates improved dispersion due to PEG grafting. Additionally, MC3T3-E1 cell culture on PCL and PCL/GO-g-PEG scaffolds provided preliminary insights into their potential for tissue engineering. In a previous study conducted by Yavuz et.al. (23), HAP was synthesized using the sol-gel method, followed by surface modification with PEG-400Si. Subsequently, nanofibrous biomembranes containing unmodified (PCL/PEG-HAp) and modified HAp (PCL/PEG-400Si-HAp) were produced via electrospinning. In vitro assessments demonstrated biocompatibility for all biomembranes, with the PCL/PEG-400Si-HAp biomembrane exhibiting notably higher cellular protein expression, approximately 1.5 times more than the PCL biomembrane, over 24 h, 48 h, and 72 h. They concluded that the electrospun biomembrane composed of PCL/PEG-400Si-HAp holds promise as a prospective candidate for applications in bone tissue engineering scaffolds. In a different study performed by Santos et. al. (24), PLGA/hydroxyapatite/β-tricalcium phosphate membranes were fabricated with two different methods (dry phase inversion and electrospinning). This investigation demonstrated the feasibility of fabricating bilayer membranes comprising PLGA, HAp, and β-TCP, which exhibited suitable in vitro degradation, a mechanical profile striking a balance between rigidity and flexibility, well-defined pore architecture and dimensions, robust interlayer bonding, and enhanced potential for bone regeneration.

The principal objective of this inquiry is to ascertain and discuss the attributes of a tissue scaffold with the potential to facilitate the restoration of functional

connections in cases of spinal cord injury. This objective involves the straightforward methodological preparation of a composite film, serving as a promising scaffold that prominently combines synthetic polymers (PLGA and PEG) with ceramic material (HAP).

2. EXPERIMENTAL

2.1. Synthesis of Hydroxyapatite

A procedure called wet precipitation was used for HAP synthesis. This method was chosen because it offers high yield, simplicity, and low cost in contrast to other methods of obtaining HAP. For HAP synthesis, a reaction of 250 mL of 0.6 M H_3PO_4 (purchased from Merck/Sigma-Aldrich, 80%) and 18.56 g $Ca(OH)_2$ (purchased from Merck/Sigma-Aldrich, 99%) was prepared, and then NaOH (purchased from Merck | Sigma-Aldrich, 99%) was added and stirred at room temperature for 7 days, keeping the pH above 11. After 7 days, the mixture was centrifuged three times for 5 min at 3000 rpm. Then, a filtration system was set up, and the mixture was poured into a Buchner funnel for separation. Finally, the obtained wet product was incubated in a dry oven at a temperature of 80 °C for 5 days. A portion of the HAP obtained during the synthesis process was sintered at 1050 °C for two hours to evaluate the effect of sintering.

2.2. Preparation of PLGA-PEG/HAP Composite Film

In this study, a PLGA-PEG/HAP composite film was prepared, wherein the central objective revolved around the attainment of a uniform dispersion of the constituent elements through a methodical process involving uncomplicated mixing and meticulous sonication. Firstly, the PLGA (purchased from Sigma Aldrich, 50:50, CAS Number: 26780-50-7, m_w 30000-60000 g/mol) and PEG (purchased from Sigma Aldrich, CAS Number: 25322-68-3, m_w ~1500) polymer solutions were prepared, incorporating a 5% polymer content by weight, while maintaining a volumetric ratio of 95% chloroform. Subsequently, equal amounts of PLGA and PEG solutions were blended until achieving a homogeneous solution at ambient temperature. In addition, a chloroform-based solution of HAP was prepared, subsequently followed by the meticulous blending of PLGA-PEG/HAP solutions at a specific proportion of 65% PLGA-PEG to 35% HAP. The mixture was left to agitate at 40 °C for 24 h and sonicated as stated in a previous report (25) where the sonication time was divided into 10 s intervals with an amplitude of 100 using a Qsonica Q700 sonicator model CL-334. The Petri dishes were enveloped within a hermetically sealed container exhibiting a substantial headspace and maintained in an immobile state until solvent evaporation ensued. Following the completion of film formation, the resulting constructs were retrieved for subsequent characterization endeavors.

2.3. Characterizations

2.3.1. Fourier-Transform Infrared Spectroscopy Analysis (FTIR)

FTIR spectra were collected for the composite films between 4000 - 650 cm^{-1} at 20 °C. The spectra were recorded and stored on an ATR (Attenuated Total Reflectance) Perkin Elmer spectrometer. Four scans were performed at 4 cm^{-1} resolution.

2.3.2. X-ray Diffraction Analyses (XRD)

The equipment used in this analysis was a Bruker 8 with a powder method. A metal sample holder was used and a small amount of sample was placed so that it covered an area 1 cm long and 3 mm wide. The sample holder was then placed inside the equipment and secured inside the equipment. The analysis conditions were then programmed in the equipment, a speed between 15 and 30 rpm was programmed. The lamp used was a copper (Cu) lamp at 30 kV. Tests were performed in the 2θ= 20-80° range and 0.02° step size.

2.3.3. Scanning electron microscopy (SEM)

Morphological examination of all prepared composite films was conducted using scanning electron microscopy (SEM; EVO LS 10, ZEISS). A metal sample holder was prepared with graphite adhesive tape, onto which a small section of the specimen was positioned. Subsequently, a fine layer of gold was deposited onto the samples via assisted deposition at approximately 1 kV for a duration of 8 minutes. The prepared samples were placed onto an electron microscope tray, and images were captured across various magnifications and distinct regions.

2.3.4. Thermogravimetric Analysis (TGA) and Differential Scanning Calorimetry (DSC) Analysis

Thermogravimetric analysis was carried out by measuring the mass change, thermal stability, and maximum decomposition temperature of all samples with increasing temperature. The test was carried out in an unsealed platinum flask using a nitrogen atmosphere at a flow rate of 20 mL/min, using a heating period of 10 °C/min from room temperature (±20 °C) to 700 °C at a flow rate of 20 mL/min. The equipment used was a Shimadzu TGA-50 model. Composite films were characterized using Shimadzu DSC model DSC-50 DSC equipment and programmed for room temperature heating (±20 °C) up to 120 °C for a period of 10 °C/min (initial run). The mass of the samples analyzed ranged from 5 to 10 mg. At the end of the run, the furnace was cooled with liquid nitrogen to a temperature of -20 °C or -30 °C.

2.3.5. In vitro cell studies

Prior to culturing, the composite films underwent a sterilization procedure. Subsequently, they were cultured in Dulbecco's Modified Eagle Medium (DMEM), which served as a nutritive medium akin to the extracellular matrix (ECM). The experimental approach employed NIH 3T3 mouse embryonic fibroblast cells, obtained subsequent to their isolation from a designated cell line. Each composite film sample was meticulously seeded with an approximate population of $7x10^4$ NIH-3T3 cell lines. At intervals of the 1st, 3rd, 5th, and 7th days within the course of cell culture, the cells were subjected to staining with Dio6 and DAPI (5 mM) dyes. Subsequent to staining, an in-depth examination of

the cellular attributes and behaviors was undertaken utilizing fluorescence microscopy.

3. RESULT AND DISCUSSION

3.1. FTIR Analysis

The purpose of this analysis is to determine the presence of both reagents in the sample. For the spectrum in Figure 1.A, the characteristic 5 signal of the PLGA structure was observed. The peak around 1765 - 1740 cm^{-1} was assigned to C=O bonds, while the signal for -C-C-O bonds was assigned between 1300 - 1080 cm^{-1}. The ether type appeared between 1085 and 1190 cm^{-1} for -C-O-C- bonds. The -CH, -CH_2 and -CH_3 stretching group of the polymer was observed around 3000 - 2900 cm^{-1}. It was assigned to methyl (-CH_3) at 1383 cm^{-1} and methylene (-CH_2) at 1423 cm^{-1}. Finally, the peaks observed around 869 cm^{-1} correspond to the C-C bond. Between 1500 and 1250 cm^{-1}, deformation of the -CH_2 and -CH_3 bond may be observed; CH and CH_2 vibrations between 1350 and 1150 cm^{-1} and stretching of the -C-O ester bonds between 1300 and 1150 cm^{-1} (26–29).

3.2. XRD Analysis

The purity and crystallinity of the synthesized HAP were evaluated by XRD. Thanks to the interaction of X-rays with HAP powders, a diffraction diagram was obtained. Since the diffraction diagram produced was considered as the fingerprint of the crystalline phase that produced it, it was possible to identify and determine whether the product obtained was really what we expected. The diffraction diagram obtained was plotted as a function of density versus angle 2θ. Figure 1.B shows the X-ray spectrum of the HAP powder. The first four peaks with the highest intensity located between the angular region 20 < 2θ < 60 were assigned indices attributed to hydroxy-apatite with Miller indices 002, 211, 112, and 300, respectively. These spectra were calculated with the structural parameters as in the previous study (30), in which a very similar behavior was observed, although the pattern presents narrower and more intense peaks. The spectra obtained were compared with JCPDS 09-432 (catalogue number) and it was proved that the sample obtained from HAP by wet precipitation method represents the typical pattern of this type of bioceramics (31–33). PLGA-PEG patterns were observed approximately at 211 and 300. PEG was observed at 211 and 202, while PLGA was observed in 211, 300, and 202 bands. When HAP bioceramic material was added to PLGA-PEG composite structures, the presence of HAP crystal structure continued to be observed at miller indices of 310, 222, 213 and, 411.

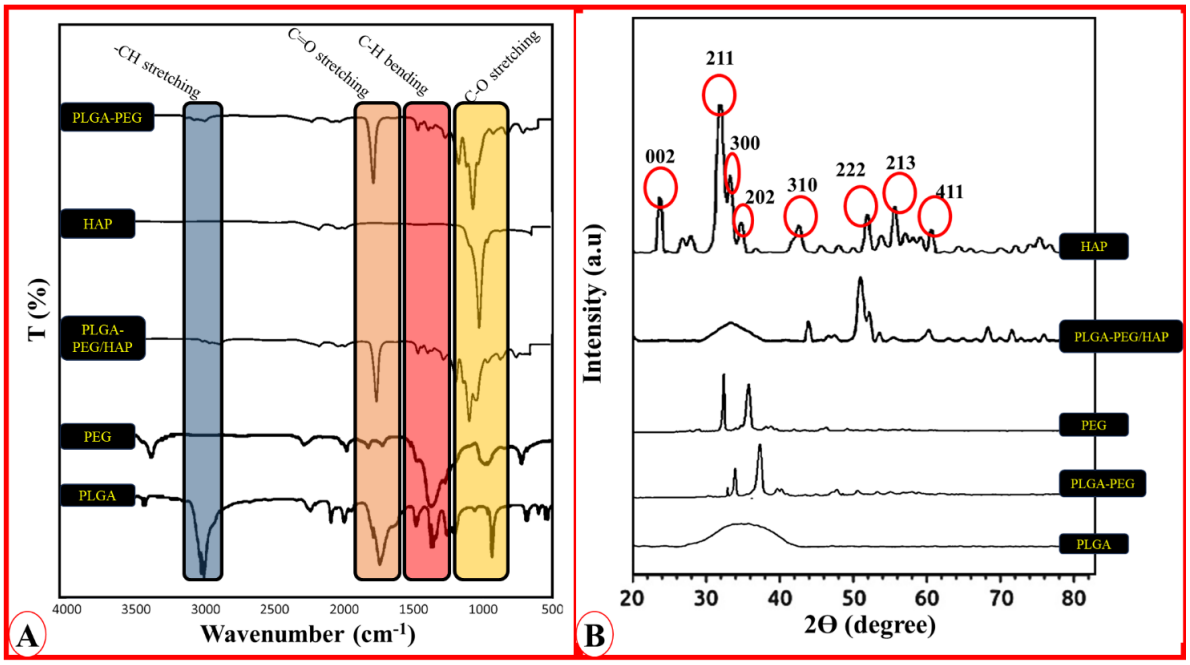

Figure 1: (A) FTIR spectra of and (B) XRD pattern of PLGA, PEG, HAP, PLGA-PEG, PLGA-PEG/HAP.

3.3. SEM Analysis

In the SEM micrographs (Figure 2), a comprehensive examination was conducted on PLGA, HAP, and the composite film system involving PLGA-PEG and HAP. Remarkably, the utilization of an amorphous manifestation of PLGA-PEG was pursued, culminating in films that exhibited a notable cohesiveness in their structural makeup. Evident in the observations was a considerably gradual film formation process, distinct from the expeditious crystalline PLGA counterpart. This variance notably influenced the dispersion profile of hydroxyapatite within the polymer matrix. Noteworthy clusters of HAP were perceptible within the SEM micrograph of the PLGA-PEG/HAP composite. However, a visual appraisal of the film's surface led to the discernment of a more uniformly distributed surface. The precise manage-ment of surface material attributes holds pivotal importance in dictating the efficacy of cell adhesion. Pertinent factors impacting the efficacy of biomaterial surfaces encompass attributes such as wettability and surface topography. Significantly, surface roughness has emerged as a pivotal facet influencing cellular adhesion dynamics. It has been suggested that certain textured configurations exhibit enhanced cellular behavior when compared to

conventional films. This interplay of surface roughness, in tandem with the surface's wettability and chemical composition, collectively orchestrates and modifies cellular affinity towards the substrate. While a meticulous quantification of surface roughness was not undertaken within this investigation, it is noteworthy that the scrutinized films exhibit a surface characterized by nuanced roughness and embellished with hydroxyapatite attributes. This material is widely renowned for its inherent wettability, biocompatibility, and osteoconductive qualities. Consequently, the films at hand demonstrate tangible potential for biomedical applications, particularly in the realm of bone-regenerative pursuits (31,34–36).

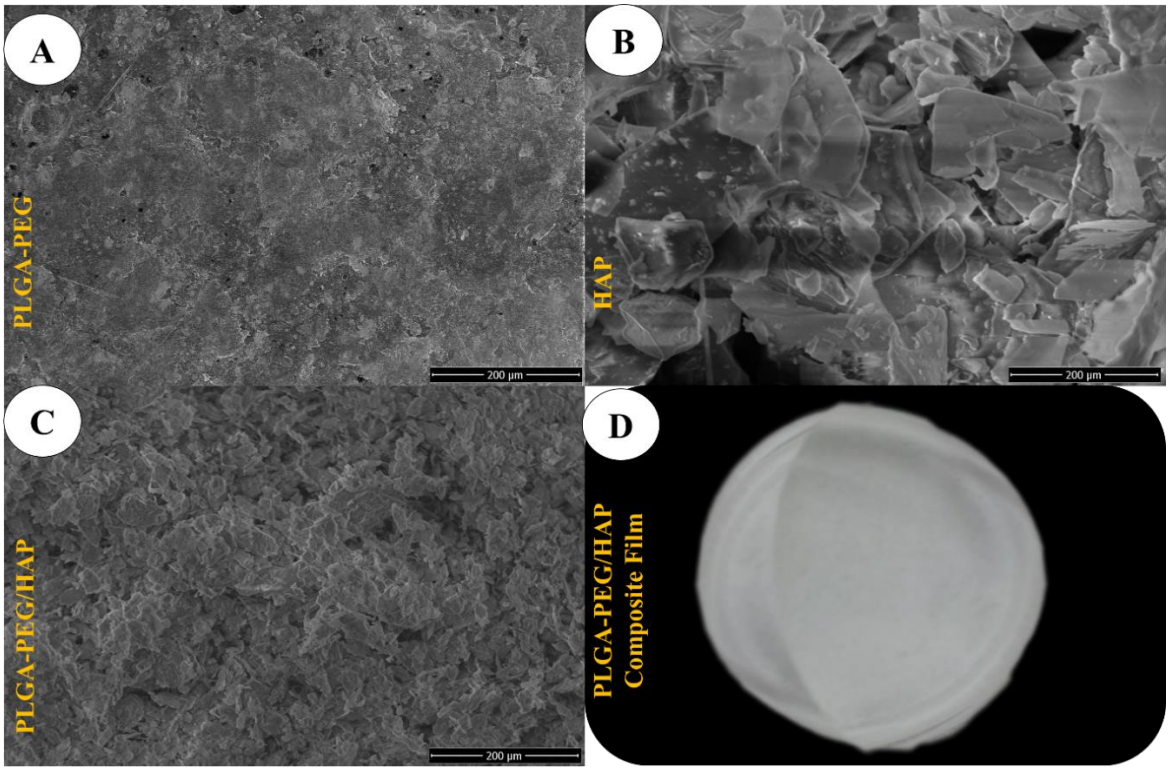

Figure 2: SEM micrographs of the surface of PLGA-PEG, HAP and PLGA-PEG/HAP composite film (Scale bar: 200 µm) and the image of PLGA-PEG/HAP composite film.

3.4. TGA and DSC Analysis

Figure 3 (B) illustrates the DSC profiles of HAP, PLGA-PEG, and PLGA-PEG/HAP composite film specimens. The determination of glass transition temperature (T_g) for PEG polymers has exhibited variability across literature sources, with certain studies acknowledging the absence of T_g for PEG polymers with low molecular weights (37). However, prevailing research generally suggests a T_g value below 35 °C for PEG (38,39). Conversely, a well-established T_g range of 50-55 °C has been attributed to PLGA 50:50 polymer (40–42). Consequently, the distinct TGA and DSC plots for the PLGA and PEG polymers employed in this investigation were omitted. Notably, the HAP sample displayed no discernible T_g or distinctive thermal point throughout the temperature ramp until 100 °C. For the PLGA-PEG composite, a T_g within the range of 37-40 °C was ascertained. These findings, in accordance with previous inquiries, align with the notion that the incorporation of PEG diminishes the T_g of the polymer blend (38,41,43). The scrutiny of the DSC profile for the PLGA-PEG/HAP composite film evinced negligible distinctions compared to the DSC profile of PLGA-PEG samples. This observation implies that the HAP sample, which lacks any apparent temperature-related characteristics upon temperature elevation to 100 °C, does not exert any influence on the thermal attributes of the PLGA-PEG blend (44). Thus, it can be inferred that the introduction of HAP into the PLGA-PEG blend exerts no alteration on the thermal traits of the composite. Moreover, a crystallization peak at approximately 72 °C was conspicuous in the DSC patterns of both PLGA-PEG and PLGA-PEG/HAP composite films, produced through a simple methodology encompassing mixing, sonication, and casting-drying stages. Thus, it can be posited that the impact of PEG and HAP content on the of the composite films parallels at the T_g crystallization temperature (43,45).

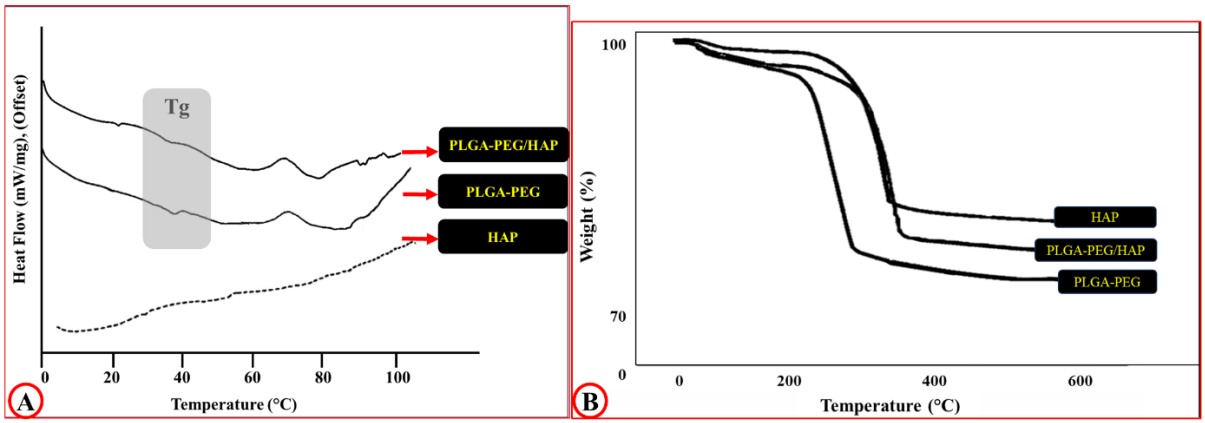

Figure 3: (A) TGA curves of and (B) DSC graph of HAP, PLGA-PEG, and PLGA-PEG/HAP.

Figure 3. (A), and Table 1. demonstrate the TGA curves and numerical data of HAP, PLGA-PEG, and PLGA-PEG/HAP samples, respectively. All specimens experienced mass loss in two different temperature zones (Region-I and Region-II). The moisture-induced mass loss values of HAP, PLGA-PEG, and PLGA-PEG/HAP samples at the first 100 degrees were determined as 0.64, 1.29, and 1.02(%), respect-tively. The total mass loss (%) in these two regions, i.e. total degradation (%), was lowest in the HAP sample and highest in the PLGA-PEG sample. This is an indication that ceramic materials have a higher thermal stability than polymeric materials. In addition, the mass loss in the PLGA-PEG/HAP sample was higher than in the HAP sample and lower than in the PLGA-PEG sample. Thus, it may be said that the thermal stability of the PLGA-PEG polymer system with the addition of HAP increases (46,47).

Table 1: The results of TGA analysis of HAP, PLGA-PEG, and PLGA-PEG/HAP.

		HAP	PLGA-PEG	PLGA-PEG/HAP
(A); Region-I (B); Region-II	Temperature Range (°C)	(A) 25-194	(A) 25-224	(A) 25-205
		(B) 194-611	(B) 224-528	(B) 200-610
	Degradation Amount (%)	(A) 2.68	(A) 3.73	(A) 3.08
		(B) 2.64	(B) 6.70	(B) 5.33
	Maximum Degradation Rate (%/min)	(A) 0.28	(A) 0.69	(A) 0.42
		(B) 0.08	(B) 0.96	(B) 0.58
	Maximum Degradation Temperature (°C)	(A) 46	(A) 182	(A) 168
		(B) 450	(B) 451	(B) 450
	Total Degradation (%)	5.96	11.72	9.43
	Remaining (%)	94.04	88.28	90.57

3.5. Cell proliferation Study

The results of cell attachment and proliferation after DAPI staining on PLGA-PEG (control) and PLGA-PEG/HAP composite films are shown in Figure 4. For the cell proliferation assay, the cell amount of the PLGA-PEG/HAP composite group was 1.8 times higher than that of the control group, PLGA-PEG, on day 7 of culture, showing a significant improvement in statistical analysis ($P < 0.05$). In particular, fewer cells proliferated in the PLGA-PEG composite film on day 7. It was concluded that HAP in the polymeric composite film was effective in the attachment and proliferation of chondrocytes (11,48–51).

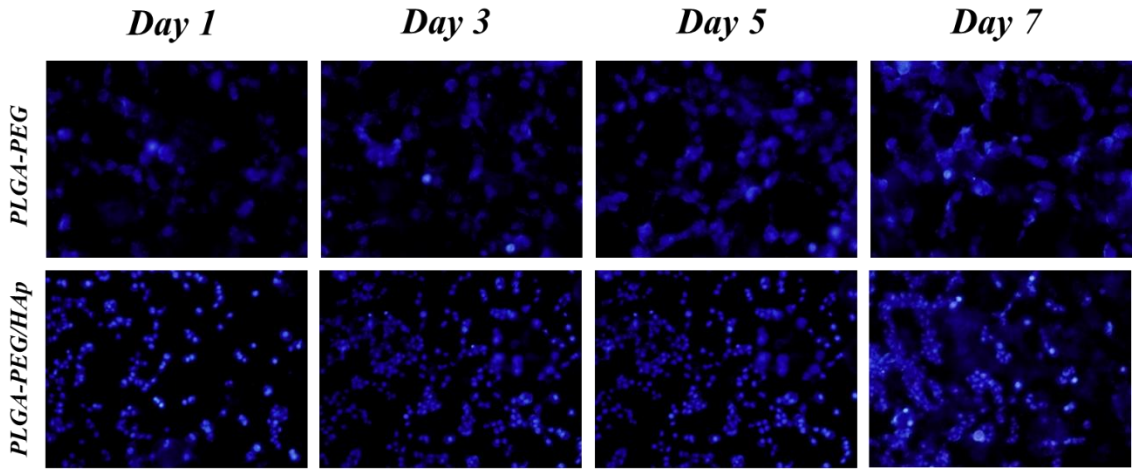

Figure 4: Cell line study florescence DAPI micrographs of 40x.

After incubation of fibroblast NIH/3T3 cells on composite films for 24 h, the behavior of cells was directly observed by fluorescence microscopy. The increase in the number of cells was clearly observed at the end of the 1st, 3rd, 5th, and 7th days, especially on the PLGA-PGE/HAP composite film. In a similar study, tissue engineered poly (lactide-co-glycolide)/polyethylene glycol (PLGA-PEG) nanofiber scaffolds were designed by electrospun technique for the treatment of spinal cord injuries. In vitro-vivo studies were performed on induced mouse embryonic fibroblasts (MEFs) reprogrammed into neural stem cells (iNSCs) using PLGA-PEG nanofibers. No difference was observed in iNSC cell viability at day 7 in PLGA and PLGA-PEG groups. Cell adhesion rates, cell proliferation and cell number on PLGA-PEG scaffolds increased steadily from day 1 to day 9 of incubation. Hoechst33342 cell nuclear staining of the sections was performed to determine the iNSCs in the PLGA-PEG scaffolds. No differences were observed in the cells within the scaffold. Hoechst staining showed core quality in the PLGA-PEG nanofiber scaffold. Nuclear staining showed that the cell population growing on the PLGA-PEG scaffold was larger than on the PLGA scaffold (52). In another previous study, PLGA and nano-hydroxyapatite (nHA)/PLGA composite scaffolds were designed as a predictive preclinical tool to study prostate cancer (mPC) and reduce the gap that exists with conventional 2D cultures. 2D and 3D cell distribution was observed using core fluorescence imaging on (nHA)/PLGA composite scaffolds. Cells were stained with Dio (green-hFOB 1.19) and Dil (red-PC-3). At the end of day 7, it was observed that hFOB: PC-3 cells were present in 2D cells. In addition, PC-3 cells were also observed equivalently. In 3D culture medium, (nHA)/PLGA scaffold colonized both hFOB 1.19 and PC-3 cells. However, more PC-3 cells were observed in the 4 mg (nHA)/PLGA scaffold group. The addition of nHA to the composite scaffolds corresponded to increased cell viability. As a result of this study, fluorescence imaging showed that PC-3 proliferated to a greater extent, and qualitatively this was more pronounced in scaffolds with higher nHA content (53).

4. CONCLUSION

This investigation successfully undertook the preparation of PLGA-PEG/HAP composite films employing a simplified fabrication methodology. The inclusion of HAP within the polymer matrix has garnered significant attention in the field of tissue engineering. XRD patterns exhibited distinctive crystalline features, affirming the quality of the resultant samples. FTIR analysis revealed salient spectral bands, notably the broad signals in the aromatic region spanning 1600 cm^{-1} to 1400 cm^{-1}, signifying the amalgamation of HAP and the polymer substrate. SEM micrographs depicted surface uniformity in the samples, attributed to the amorphous nature of the polymer. This amorphicity retards matrix formation, thereby promoting efficient filler dispersion. Further enhancement was achieved through sonication, accentuating filler distribution within the polymeric matrix. Consequently, the production methodology's potential for ensuring reproducibility in terms of surface morphology and chemical composition becomes evident, presenting prospects for medical applications. TGA disclosed a maximum material loss of around ~9.5% in the PLGA-PEG/HAP composite film. This outcome validates the feasibility of autoclave sterilization for applications necessitating sterile substrates. In the DSC curve, a discrete yet broad transition within the 25-40 °C temperature range indicated the composite material's glass transition region. Integrating cellular assays and DAPI staining demonstrated the composite film's propensity for promoting cell adhesion in tissue engineering scenarios, while concurrently exhibiting minimal cytotoxic effects. Anticipated forthcoming research endeavors encompasssing comprehensive biocompatibility assessments, degradation kinetics, and in vivo animal experimentation will provide a more nuanced understanding, substantiating the applicability of these composite films within the domain of bone tissue engineering.

5. CONFLICT OF INTEREST

The authors declare no potential conflict of interest.

6. REFERENCES

1. Ozder MN, Ciftci F, Rencuzogullari O, Arisan ED, Ustündag CB. In situ synthesis and cell line studies of nano-hydroxyapatite/graphene oxide composite materials for bone support applications. Ceram Int [Internet]. 2023 May 1;49(9):14791–803. Available from: <URL>.

2. Yuan B, Chen H, Zhao R, Deng X, Chen G, Yang X, et al. Construction of a magnesium hydroxide/graphene oxide/hydroxyapatite composite coating on Mg–Ca–Zn–Ag alloy to inhibit bacterial infection and promote bone regeneration. Bioact Mater [Internet]. 2022 Dec 1;18:354–67. Available from: <URL>.

3. Taylor EC, Fitzpatrick CE, Thompson SE, Justice SB. Acute Traumatic Spinal Cord Injury. Adv Emerg Nurs J [Internet]. 2022 Oct 1;44(4):272–80. Available from: <URL>.

4. Serafin A, Rubio MC, Carsi M, Ortiz-Serna P, Sanchis MJ, Garg AK, et al. Electroconductive PEDOT nanoparticle integrated scaffolds for spinal cord tissue repair. Biomater Res [Internet]. 2022 Nov 22;26(1):63. Available from: <URL>.

5. Ma Y, Chen Q, Li W, Su H, Li S, Zhu Y, et al. Spinal cord conduits for spinal cord injury regeneration. Eng Regen [Internet]. 2023 Mar 1;4(1):68–80. Available from: <URL>.

6. Pourkhodadad S, Hosseinkazemi H, Bonakdar S, Nekounam H. Biomimetic engineered approaches for neural tissue engineering: Spinal cord injury. J Biomed Mater Res Part B Appl Biomater [Internet]. 2023 Mar 10;111(3):701–16. Available from: <URL>.

7. Wang M, Xu P, Lei B. Engineering multifunctional bioactive citrate-based biomaterials for tissue engineering. Bioact Mater [Internet]. 2023 Jan;19:511–37. Available from: <URL>.

8. Sun F, Sun X, Wang H, Li C, Zhao Y, Tian J, et al. Application of 3D-Printed, PLGA-Based Scaffolds in Bone Tissue Engineering. Int J Mol Sci [Internet]. 2022 May 23;23(10):5831. Available from: <URL>.

9. Makadia HK, Siegel SJ. Poly Lactic-co-Glycolic Acid (PLGA) as Biodegradable Controlled Drug Delivery Carrier. Polymers (Basel) [Internet]. 2011 Aug 26;3(3):1377–97. Available from: <URL>.

10. Wang Z, Cui K, Costabel U, Zhang X. Nanotechnology-facilitated vaccine development during the coronavirus disease 2019 (COVID-19) pandemic. Exploration [Internet]. 2022 Oct 21;2(5):20210082. Available from: <URL>.

11. Wei J, Yan Y, Gao J, Li Y, Wang R, Wang J, et al. 3D-printed hydroxyapatite microspheres reinforced PLGA scaffolds for bone regeneration. Biomater Adv [Internet]. 2022 Feb;133:112618. Available from: <URL>.

12. Shabani Z, Rahbarghazi R, Karimipour M, Ghadiri T, Salehi R, Sadigh-Eteghad S, et al. Transplantation of bioengineered Reelin-loaded PLGA/PEG micelles can accelerate neural tissue regeneration in photothrombotic stroke model of mouse. Bioeng Transl Med [Internet]. 2022 Jan 29;7(1):e10264. Available from: <URL>.

13. Lin C-C, Anseth KS. PEG Hydrogels for the Controlled Release of Biomolecules in Regenerative Medicine. Pharm Res [Internet]. 2009 Mar 18;26(3):631–43. Available from: <URL>.

14. Mikhail AS, Ranger JJ, Liu L, Longenecker R, Thompson DB, Sheardown HD, et al. Rapid and Efficient Assembly of Functional Silicone Surfaces Protected by PEG: Cell Adhesion to Peptide-Modified PDMS. J Biomater Sci Polym Ed [Internet]. 2010 Jan 2;21(6–7):821–42. Available from: <URL>.

15. Wang P, Wang H, Ma K, Wang S, Yang C, Mu N, et al. Novel cytokine-loaded PCL-PEG scaffold composites for spinal cord injury repair. RSC Adv [Internet]. 2020;10(11):6306–14. Available from: <URL>.

16. Xu L, Wang Y-Y, Huang J, Chen C-Y, Wang Z-X, Xie H. Silver nanoparticles: Synthesis, medical applications and biosafety. Theranostics [Internet]. 2020;10(20):8996–9031. Available from: <URL>.

17. Ielo I, Calabrese G, De Luca G, Conoci S. Recent Advances in Hydroxyapatite-Based Biocomposites for Bone Tissue Regeneration in Orthopedics. Int J Mol Sci [Internet]. 2022 Aug 27;23(17):9721. Available from: <URL>.

18. Jianfei H, Fuke W, Guiran Y, Xinyu L, Di J, Dejian L. Application advantages of hydroxyapatite surface modification as a bone scaffold for tissue engineering. Chinese J Tissue Eng Res [Internet]. 2022 Apr 8;26(10):1610–4. Available from: <URL>.

19. Aminatun, Suciati T, Sari YW, Sari M, Alamsyah KA, Purnamasari W, et al. Biopolymer-based polycaprolactone-hydroxyapatite scaffolds for bone tissue engineering. Int J Polym Mater Polym Biomater [Internet]. 2023 Mar 24;72(5):376–85. Available from: <URL>.

20. Fiume E, Magnaterra G, Rahdar A, Verné E, Baino F. Hydroxyapatite for Biomedical Applications: A Short Overview. Ceramics [Internet]. 2021 Sep 28;4(4):542–63. Available from: <URL>.

21. Farag MM. Recent trends on biomaterials for tissue regeneration applications: review. J Mater Sci [Internet]. 2023 Jan 1;58(2):527–58. Available from: <URL>.

22. Scaffaro R, Lopresti F, Maio A, Botta L, Rigogliuso S, Ghersi G. Electrospun PCL/GO-g-PEG structures: Processing-morphology-properties relationships. Compos Part A Appl Sci Manuf [Internet]. 2017 Jan;92:97–107. Available from: <URL>.

23. Yavuz E, Erdem R, Küçüksayan E, Akarsu E, Akarsu M. Preparation and Characterization of Polyethylene Glycol Functional Hydroxyapatite/Polycaprolactone Electrospun Biomembranes for Bone Tissue Engineering Applications. Fibers Polym [Internet]. 2021 May 27;22(5):1274–84. Available from: <URL>.

24. dos Santos VI, Merlini C, Aragones Á, Cesca K, Fredel MC. In vitro evaluation of bilayer membranes of PLGA/hydroxyapatite/β-tricalcium phosphate for guided bone regeneration. Mater Sci Eng C [Internet]. 2020 Jul;112:110849. Available from: <URL>.

25. Álvarez-Suarez AS, López-Maldonado EA, Graeve OA, Martinez-Pallares F, Gómez-Pineda LE, Oropeza-Guzmán MT, et al. Fabrication of porous polymeric structures using a simple sonication technique for tissue engineering. J Polym Eng [Internet]. 2017 Nov 27;37(9):943–51. Available from: <URL>.

26. Liu X, Ma Y, Chen M, Ji J, Zhu Y, Zhu Q, et al. Ba/Mg co-doped hydroxyapatite/PLGA composites enhance X-ray imaging and bone defect regeneration. J Mater Chem B [Internet]. 2021;9(33):6691–702. Available from: <URL>.

27. Liao S, Watari F, Zhu Y, Uo M, Akasaka T, Wang W, et al. The degradation of the three layered nano-carbonated hydroxyapatite/collagen/PLGA composite membrane in vitro. Dent Mater [Internet]. 2007 Sep;23(9):1120–8. Available from: <URL>.

28. Lee JB, Lee SH, Yu SM, Park J-C, Choi JB, Kim JK. PLGA scaffold incorporated with hydroxyapatite for cartilage regeneration. Surf Coatings Technol [Internet]. 2008 Aug;202(22–23):5757–61. Available from: <URL>.

29. Qian J, Xu W, Yong X, Jin X, Zhang W. Fabrication and in vitro biocompatibility of biomorphic PLGA/nHA composite scaffolds for bone tissue engineering. Mater Sci Eng C [Internet]. 2014 Mar;36:95–101. Available from: <URL>.

30. Yelten-Yilmaz A, Yilmaz S. Wet chemical precipitation synthesis of hydroxyapatite (HA) powders. Ceram Int [Internet]. 2018 Jun;44(8):9703–10. Available from: <URL>.

31. Hassan M, Sulaiman M, Yuvaraju PD, Galiwango E, Rehman I ur, Al-Marzouqi AH, et al. Biomimetic PLGA/Strontium-Zinc Nano Hydroxyapatite Composite Scaffolds for Bone Regeneration. J Funct Biomater [Internet]. 2022 Jan 28;13(1):13. Available from: <URL>.

32. Yuan B, Zhang Y, Wang Q, Ren G, Wang Y, Zhou S, et al. Thermosensitive vancomycin@PLGA-PEG-PLGA/HA hydrogel as an all-in-one treatment for osteomyelitis. Int J Pharm [Internet]. 2022 Nov;627:122225. Available from: <URL>.

33. Liuyun J, Chengdong X, Lixin J, Lijuan X. Degradation behavior of hydroxyapatite/poly(lactic-co-glycolic) acid nanocomposite in simulated body fluid. Mater Res Bull [Internet]. 2013 Oct;48(10):4186–90. Available from: <URL>.

34. Chang P-C, Luo H-T, Lin Z-J, Tai W-C, Chang C-H, Chang Y-C, et al. Preclinical evaluation of a 3D-printed hydroxyapatite/poly(lactic-co-glycolic acid) scaffold for ridge augmentation. J Formos Med Assoc [Internet]. 2021 Apr;120(4):1100–7. Available from: <URL>.

35. Jiang L, Li Y, Xiong C, Su S. Preparation and characterization of a novel degradable nano-

hydroxyapatite/poly(lactic- co -glycolic) composite reinforced with bamboo fiber. Mater Sci Eng C [Internet]. 2017 Jun;75:1014–8. Available from: <URL>.

36. Selvaraju S, Ramalingam S, Rao JR. Inorganic apatite nanomaterial: Modified surface phenomena and its role in developing collagen based polymeric bio-composite (Coll-PLGA/HAp) for biological applications. Colloids Surfaces B Biointerfaces [Internet]. 2018 Dec;172:734–42. Available from: <URL>.

37. Zhu KJ, Xiangzhou L, Shilin Y. Preparation, characterization, and properties of polylactide (PLA)–poly(ethylene glycol) (PEG) copolymers: A potential drug carrier. J Appl Polym Sci [Internet]. 1990 Jan 5;39(1):1–9. Available from: <URL>.

38. Pişkin E, Kaitian X, Denkbaş EB, Küçükyavuz Z. Novel PDLLA/PEG copolymer micelles as drug carriers. J Biomater Sci Polym Ed [Internet]. 1996 Jan 2;7(4):359–73. Available from: <URL>.

39. Zheng F, Wang C, Huang K, Li J. Surface Adsorption in PEG/Hydroxyapatite and PEG/Dickite Composite Phase Change Materials. Energy & Fuels [Internet]. 2021 Jul 1;35(13):10850–9. Available from: <URL>.

40. Xu XF. Preparation and *In Vitro* Degradation of PLGA/HA Composite Fiber Scaffolds by Electrospinning. Adv Mater Res [Internet]. 2012 Nov;591–593:982–8. Available from: <URL>.

41. Vega E, Egea, Calpena, Espina, García. Role of hydroxypropyl-β-cyclodextrin on freeze-dried and gamma-irradiated PLGA and PLGA–PEG diblock copolymer nanospheres for ophthalmic flurbiprofen delivery. Int J Nanomedicine [Internet]. 2012 Mar;2012(7):1357–71. Available from: <URL>.

42. Park J-W, Hwang J-U, Back J-H, Jang S-W, Kim H-J, Kim P-S, et al. High strength PLGA/Hydroxyapatite composites with tunable surface structure using PLGA direct grafting method for orthopedic implants. Compos Part B Eng [Internet]. 2019 Dec;178:107449. Available from: <URL>.

43. Sheth M, Kumar RA, Dave V, Gross RA, McCarthy SP. Biodegradable polymer blends of poly(lactic acid) and poly(ethylene glycol). J Appl Polym Sci [Internet]. 1997 Nov 21;66(8):1495–505. Available from: <URL>.

44. Nedaipour F, Bagheri H, Mohammadi S. "Polylactic acid-polyethylene glycol-hydroxyapatite composite" an efficient composition for interference screws. Nanocomposites [Internet]. 2020 Jul 2;6(3):99–110. Available from: <URL>.

45. Ferri J, Gisbert I, García-Sanoguera D, Reig M, Balart R. The effect of beta-tricalcium phosphate on mechanical and thermal performances of poly(lactic acid). J Compos Mater [Internet]. 2016 Dec 28;50(30):4189–98. Available from: <URL>.

46. Tukulula M, Hayeshi R, Fonteh P, Meyer D, Ndamase A, Madziva MT, et al. Curdlan-Conjugated PLGA Nanoparticles Possess Macrophage Stimulant Activity and Drug Delivery Capabilities. Pharm Res [Internet]. 2015 Feb 28;32:2713–6. Available from: <URL>.

47. Cañas-Gutiérrez A, Toro L, Fornaguera C, Borrós S, Osorio M, Castro-Herazo C, et al. Biomineralization in Three-Dimensional Scaffolds Based on Bacterial Nanocellulose for Bone Tissue Engineering: Feature Characterization and Stem Cell Differentiation. Polymers (Basel) [Internet]. 2023 Apr 24;15(9):2012. Available from: <URL>.

48. Yang X, Li Y, He W, Huang Q, Zhang R, Feng Q. Hydroxyapatite/collagen coating on PLGA electrospun fibers for osteogenic differentiation of bone marrow mesenchymal stem cells. J Biomed Mater Res Part A [Internet]. 2018 Nov 5;106(11):2863–70. Available from: <URL>.

49. Zhao Z, Ma X, Ma J, Kang J, Zhang Y, Guo Y. Sustained release of naringin from silk-fibroin-nanohydroxyapatite scaffold for the enhancement of bone regeneration. Mater Today Bio [Internet]. 2022 Jan;13:100206. Available from: <URL>.

50. Espitia-Quiroz LC, Fernández-Orjuela AL, Anaya-Sampayo LM, Acosta-Gómez AP, Sequeda-Castañeda LG, Gutiérrez-Prieto SJ, et al. Viability and Adhesion of Periodontal Ligament Fibroblasts on a Hydroxyapatite Scaffold Combined with Collagen, Polylactic Acid–Polyglycolic Acid Copolymer and Platelet-Rich Fibrin: A Preclinical Pilot Study. Dent J [Internet]. 2022 Sep 6;10(9):167. Available from: <URL>.

51. Shahabi S, Najafi F, Majdabadi A, Hooshmand T, Haghbin Nazarpak M, Karimi B, et al. Effect of Gamma Irradiation on Structural and Biological Properties of a PLGA-PEG-Hydroxyapatite Composite. Sci World J [Internet]. 2014;2014:420616. Available from: <URL>.

52. Liu C, Huang Y, Pang M, Yang Y, Li S, Liu L, et al. Tissue-Engineered Regeneration of Completely Transected Spinal Cord Using Induced Neural Stem Cells and Gelatin-Electrospun Poly (Lactide-Co-Glycolide)/Polyethylene Glycol Scaffolds. Sensebé L, editor. PLoS One [Internet]. 2015 Mar 24;10(3):e0117709. Available from: <URL>.

53. Dozzo A, Chullipalliyalil K, McAuliffe M, O'Driscoll CM, Ryan KB. Nano-Hydroxyapatite/PLGA Mixed Scaffolds as a Tool for Drug Development and to Study Metastatic Prostate Cancer in the Bone. Pharmaceutics [Internet]. 2023 Jan 11;15(1):242. Available from: <URL>.